Discharge instabilities initiated by nonuniform laser extraction in electron-beam sustained discharge KrF lasers[a)]

Mark J. Kushner
University of Illinois, Department of Electrical and Computer Engineering, Gaseous Electronics Laboratory, 607 East Healey, Champaign, Illinois 61820

(Received 17 December 1986; accepted for publication 6 February 1987)

The photon energy of KrF lasers ($\lambda = 248$ nm) is sufficiently large to photodetach electrons from the halogen negative ion (F^-) and to photoionize excited states of krypton. In electron-beam (e-beam) sustained discharge KrF lasers, the contribution of photogenerated electrons to the total rate of ionization can be large enough to significantly perturb the conductivity of the plasma. If laser oscillation is spatially nonuniform, the photoelectron contribution to the conductivity deforms the local electric field. This condition can ultimately lead to a local discharge ionization instability and an arclike termination of the discharge. In this paper, the effect of nonuniform optical extraction on the discharge stability of an e-beam sustained discharge KrF laser will be studied with results from a two-dimensional time-dependent discharge kinetics and laser extraction model. Examples of stable and unstable configurations will be presented. The time at which the arclike ionization instability terminates the discharge correlates with the time that multistep ionization becomes an appreciable fraction of the total rate of ionization . A criterion for discharge stability is proposed; gradients in conductivity caused by photogenerated electrons must be either perpendicular or parallel to the bulk electric field.

I. INTRODUCTION

Electron-beam sustained discharge (EBSD) KrF excimer lasers have long held the promise of higher efficiency than their electron-beam pumped (EBP) counterparts.[1-10] This promise originates from the supposition that EBSD KrF lasers will operate dominantly through the neutral excitation channel ($Kr^* + F_2 > KrF^* + F$), having an intrinsic efficiency of 50% whereas EBP lasers operate dominantly through the ion excitation channel($Kr^+ + F^- > KrF^*$), which has an intrinsic efficiency of 28%. EBSD lasers, though, have failed to demonstrate higher efficiency, a condition which has been partly explained by the occurrence of ionization instabilities when multistep ionization of the excited states of the rare gas become a fractionally large source of ionization.[1,3,6] Under these conditions, the balance between ionization and attachment is no longer controlled by the electron beam. The increase in electron density is then proportional to the square of the electron density, a condition which is unstable.

In an EBSD, one desires to balance the rate of ionization by the rate of attachment. In an EBSD KrF laser, ionization of Kr (and Ar for an argon buffered mix) by the e beam is balanced by dissociative electron attachment to the halogen donor, typically F_2 or NF_3. The rate of ionization, though, has contributions from other than the e beam. The change in electron density, n_e, is approximately

$$\frac{dn_e}{dt} = S_{eb} + n_e r_{0I} N_0 + n_e^2 r_{01} r_{1I} N_0 \tau - n_e r_a N_a + \phi(\sigma_a N^- + \sigma_1 N_1). \quad (1)$$

In Eq. (1), r_{0I} is the rate constant for electron impact ionization of the ground state of the noble gas (N_0), r_{01} is the rate constant for excitation to the metastable states, r_{1I} is the electron impact rate constant for ionization of the metastable states, τ is the collisional lifetime of the metastable states, r_a is the rate constant for attachment to the halogen donor (N_a), and ϕ is the photon flux. The cross sections for photodetachment of electrons from the halogen negative ion (N^-) and photoionization of excited states of the noble gas (N_1) are σ_a [5.4×10^{-18} cm^2 (Ref. 11) for F^-] and σ_1 [1.0×10^{-19} cm^2 for Kr($5s$) (Ref. 12), 5.4×10^{-18} cm^2 for Kr($5p$) (Ref. 13)], respectively. The terms in Eq. (1) are for ionization by the e beam (S_{eb}), ionization of the ground state by bulk electrons, multistep ionization of the metastable states of the noble gas, electron attachment, and photogenerated electrons. Quasisteady stable operation of the EBSD can only be sustained as long as the term for multistep ionization in Eq. (1) is locally small compared to that for ionization by the e beam. If photodetachment and photoionization, though, locally increase the electron density of one region of the discharge with respect to another, then multistep ionization will become fractionally large at that locale more rapidly than where the laser flux does not photogenerate electrons. As that region is more conductive, power deposition concentrates in the region, resulting in an ionization instability and an arclike termination of the discharge.

In this paper, the initiation of plasma ionization instabilities by nonuniform laser extraction in EBSD KrF lasers will be examined with results from a multidimensional computer model. We will show that nonuniform laser extraction, and the resultant increase in electron density due to photodetachment and photoionization, changes the plasma conductivity to a sufficient extent to deform the local electric field and change the manner of power deposition. A criterion for discharge stability is proposed; gradients in conductivity

[a)] Work supported by Los Alamos National Laboratory (Contract No. 9-X65-W1478) and the National Center for Supercomputing Applications at the University of Illinois.

 0021-8979/87/130101-07$02.40

caused by photogenerated electrons across well-defined boundaries must be either perpendicular or parallel to the bulk electric field. In Sec. II, scaling laws are discussed for EBSD lasers. In Sec. III, the EBSD KrF laser model is briefly described. Examples of stable and unstable EBSDs with nonuniform laser extraction are discussed in Sec. IV, followed by concluding remarks in Sec. V.

II. SCALING LAWS FOR EBSD LASERS

An EBSD laser differs from an EBP laser in that the majority of power is deposited by joule heating of the discharge rather than by the slowing down of beam electrons. The ratio of discharge power to e-beam power is called the discharge enhancement ratio η. Large values of η are 5–8. Therefore, local power deposition is largely determined by the local value of the discharge electric field. The local value of electric field is determined by the requirement for current continuity, $\nabla\cdot\mathbf{j} = \nabla\cdot\sigma\mathbf{E} = 0$, where j is the current density, σ is the conductivity, and E is the electric field. Expanding this expression we have

$$\nabla\sigma\cdot\mathbf{E} + \sigma\nabla\cdot\mathbf{E} = 0. \tag{2}$$

To a first approximation, Eq. (2) can be written as $\Delta\sigma/\sigma \simeq -\Delta E/E$. That is, the local relative change in electric field is approximately equal to the local relative change in conductivity. Since the electron collision frequency changes little over the parameter space of interest, $\sigma \sim n_e$. For the moment, ignore multistep ionization and assume that ionization by electrons is due to the slowing down of the e beam and is spatially uniform. For these conditions perturbations in conductivity are due to photogenerated electrons. Therefore, the relative change in electric field resulting from photogenerated electrons is approximately given by

$$\Delta E/E \simeq \frac{(\text{rate of generation of photoelectrons})}{(\text{rate of ionization by } e \text{ beam})}. \tag{3}$$

The rate of photoionization is approximately $\phi(\sigma_a[\mathrm{F}^-] + \sigma_{1(5s)}[\mathrm{Kr}(5s)] + \sigma_{1(5p)}[\mathrm{Kr}(5p)])$, where ϕ is the intracavity laser flux, and for typical discharge conditions $[\mathrm{F}^-] = 10^{14}\ \mathrm{cm}^{-3}$, $[\mathrm{Kr}(5s)] = 10^{15}\ \mathrm{cm}^{-3}$, and $[\mathrm{Kr}(5p)] = 10^{14}\ \mathrm{cm}^{-3}$. The rate of ionization by the electron beam is P_{eb}/W, where P_{eb} is the power deposited by the electron beam and W is the energy expended per ion pair (~ 25 eV). Expressing the intracavity laser flux in units of the laser saturation intensity ($\phi_s \simeq 450\ \mathrm{kW\ cm}^{-2}$) and P_{eb} in units of $\mathrm{kW\ cm}^{-3}$, we have

$$\Delta E/E \simeq 3\phi/P_{eb}. \tag{4}$$

For a total power deposition of $150\ \mathrm{kW\ cm}^{-3}$ and a discharge enhancement of $\eta = 5$, $P_{eb} = 30\ \mathrm{kW\ cm}^{-3}$. A 10% change in the local electric field, therefore, requires a laser flux equal only to the laser saturation intensity, the value which is also required for high extraction efficiency.

This scaling argument implies that if the local laser flux differs across a boundary by the saturation flux, the electric field will be significantly perturbed. The stability of the discharge then depends upon whether the new configuration of the electric field is itself stable, particularly when multistep ionization begins to dominate and perturbations in electron density are magnified by the square of the electron density.

A general design rule for discharge stability against photogenerated changes in conductivity can be quickly obtained from Eq. (2) by noting that for uniform conductivity (presumably a stable condition), we have $\sigma\nabla\cdot E = 0$. To insure that the electric field is not perturbed significantly from this configuration, we must then have that $\nabla\sigma\cdot\mathbf{E} = 0$; that is, gradients in the conductivity caused by photoelectrons are perpendicular to the electric field. An exception to this criterion is $\nabla\sigma \| \mathbf{E}$; that is, the gradient in conductivity resulting from photoelectrons is parallel to the electric field. With this constraint, the configuration can be viewed as being one-dimensional, a condition which is inherently stable to changes in the electric field providing that the rate of ionization scales as a positive power of the electric field. This can be shown by writing

$$\frac{dn_e}{dt} = n_e N k_0 (E - E_0)^m, \quad E = E_0 (n_e/n_{e0}), \tag{5}$$

where E_0 and n_{e0} are the electric field and electron density under stable conditions and $m > 0$. If the change in electric field from E_0 is small, then

$$\frac{dn_e}{dt} = n_e N k_0 \frac{E}{E_0}\left(1 - m\frac{E_0}{E}\right) = n_e N k_0\left(1 - \frac{m n_e}{n_{e0}}\right). \tag{6}$$

Since $dn_e/dt \sim -\Delta n_e$, perturbations in the electric field are stable with respect changes in the electron density provided that gradients in conductivity are parallel to the electric field.

The stability criteria discussed here apply to the change in conductivity caused by photogenerated electrons across the boundary of a region where the laser intensity is fairly uniform and a region where laser oscillation does not occur. If the change in conductivity caused by photogenerated electrons has complex spatial dependence or is nonuniform within the extraction volume, then these criteria can only be used as guides. For example, a sinusoidal ripple in conductivity caused by a series of narrow vertical stripes of laser flux will lead to filamentation and arcing in spite of satisfying the criterion that $\nabla\sigma\cdot\mathbf{E} = 0$.

III. DESCRIPTION OF THE EBSD KrF LASER MODEL

To investigate the effect of nonuniform laser extraction on the stability of EBSD KrF lasers, a discharge kinetics and laser extraction model was parametrized. This model is quite similar to that described in detail in Ref. 14. Therefore, the mechanics of the model will only be briefly discussed.

The model is a time-dependent two-dimensional computer simulation of an EBSD KrF laser. The model includes a self-consistent description of the electrical discharge circuitry, plasma chemistry, electron kinetics, and laser extraction. Electron impact rate coefficients are obtained by solution of Boltzmann's equation using the local electric field approximation. Electron-electron collisions, and collisions of electrons with excited states of the noble gas are included in the solution. The local electric field is obtained by solving

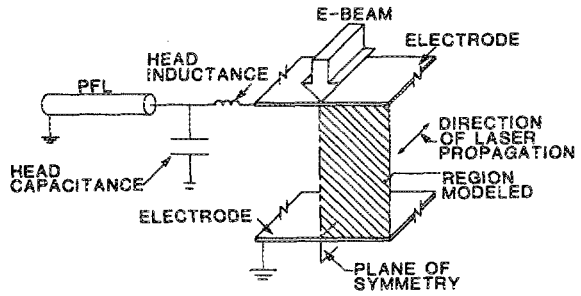

FIG. 1. Schematic of the *e*-beam sustained-discharge KrF laser used in this study. The discharge and *e*-beam parameters are listed in Table I. The *e* beam is incident through the upper (cathode) electrode. The two-dimensional model simulates values in the crosshatched region, which is symmetric across the midplane of the discharge.

TABLE I. EBSD laser operating conditions.

Gas mix	$Kr/F_2/NF_3 = 99/0.5/0.5$
Gas pressure	0.8 atm
Discharge dimensions	9 cm (gap) × 8 cm (width) × 100 cm (length)
Distance between mirrors	150 cm
Mirror reflectivities	0.6/0.95
Pulse forming line	
Length	300 ns
Impendance	1 Ω
Voltage	100 kV
E-beam power	35 kW cm^{-3} (average)

Eq. (2) by the method of successive-over-relaxation.[15] The power deposition by the *e* beam is a specified function of position and time. The geometry used for this study is shown in Fig. 1. The *e* beam is incident through the upper electrode. The discharge is symmetric across the midplane. Therefore, the plots which follow are only for the crosshatched region indicated in the figure. A single case (current pulse length of 200 ns) typically required the equivalent of 5–8 h of CPU time on a VAX-11/780 computer.

The discharge conditions for the cases discussed below are listed in Table I. The gas mixture and pressure were chosen after a parametric survey as being the values which maximize both the discharge power enhancement and laser efficiency. The discharge enhancements for the examples discussed below are 6–7 based on power actually deposited in the gas.

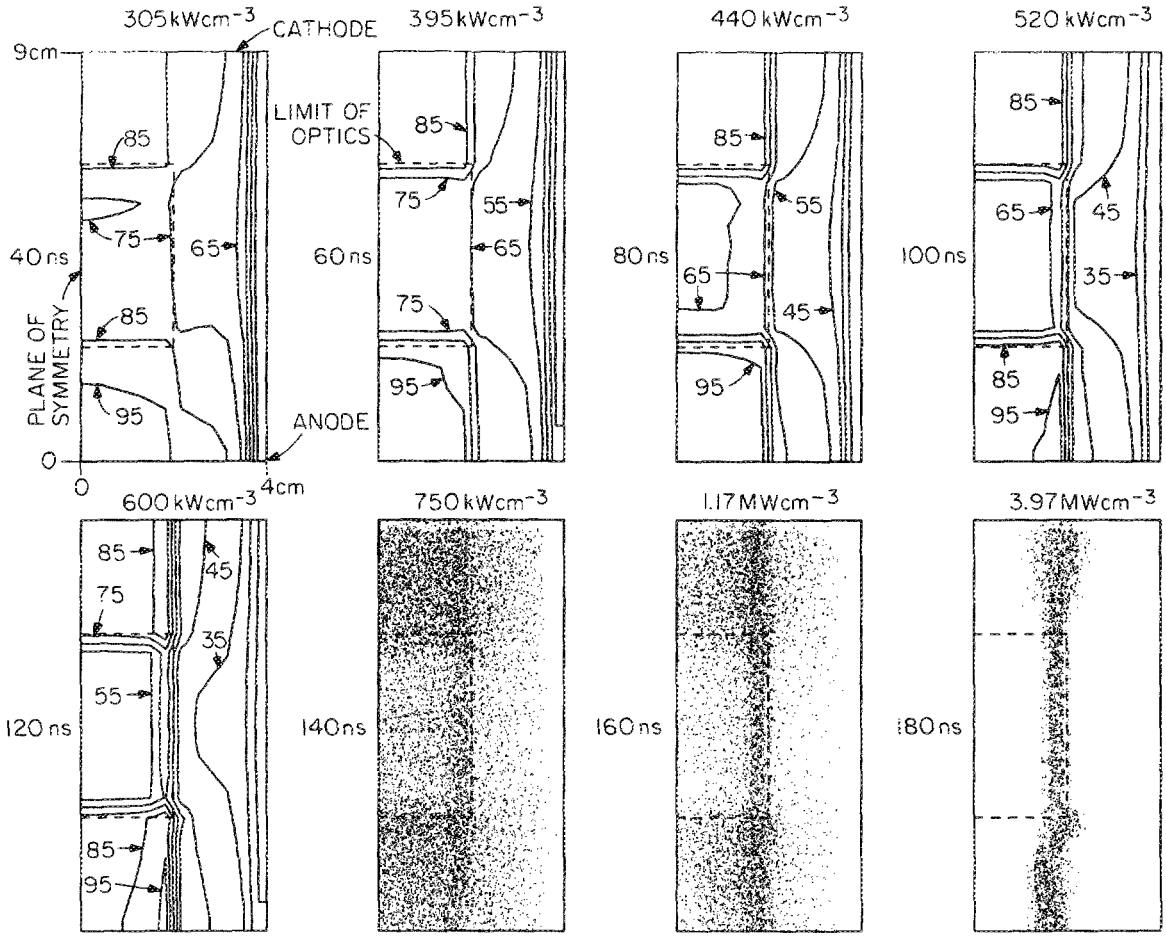

FIG. 2. Power deposition (*e* beam and discharge) for various times after the start of the current pulse in an EBSD KrF laser for the condition in Table I. The discharge aperture is 9 cm (gap) × 8 cm (width) and is symmetic across the midplane. The laser mirrors are square and centered in the discharge; laser oscillation is restricted to the volume within the dotted lines. The contour labels are power deposition as a percent of the indicated maximum value. The relative power deposition in the last three frames is given by the density of dots.

IV. NONUNIFORM LASER EXTRACTION AND DISCHARGE IONIZATION INSTABILITIES

To illustrate the effect of nonuniform laser extraction, an EBSD KrF laser having a square mirror smaller than the discharge aperture was modeled. The laser cavity overlaps only the area within the dotted lines in Fig. 2 and laser extraction is restricted to this volume. Total power deposition (e beam and discharge) for the conditions in Table I is plotted in Fig. 2 as a function of position at 20–40-ns intervals during the current pulse. The electric field vectors corresponding to the power deposition in Fig. 2 are plotted in Fig. 3.

The laser reaches threshold approximately at the time of the first frame in Figs. 2 and 3. The intracavity laser intensity after this time is approximately 7 MW/cm^2 and is nearly uniform within the extraction area. As photoelectrons are generated, the electron density increases within the extraction region relative to that outside the region. The contributions of photodetachment and photoionization are approximately equal. Since the local electric field, for constant current density, is inversely proportional to the conductivity and hence electron density, the electric field within the laser extraction volume decreases and that outside the volume increases proportionally. Recall that the majority of power deposition is by joule heating ($\mathbf{j}\cdot\mathbf{E}$) rather than by slowing down of the e beam. Therefore, power deposition and the electron temperature within the laser extraction volume also decrease. At $t = 120$ ns, the electron density and temperature within the extraction volume are 1.4×10^{14} cm^{-3} and 2.8 eV, whereas adjacent to the extraction volume the values are 0.3–1.1×10^{14} cm^{-3} and 3.1 eV, respectively.

As the difference in electron density between the extraction volume and the exterior grows larger, the extraction volume begins to resemble a conductor with respect to the exterior. The electric field is then partially excluded from the extraction region, as shown in Fig. 3. Electric field enhancement also begins to occur at the corners of the extraction volume. This condition is relatively stable until 160 ns because ionization is still dominated by the e beam. Therefore, ionization is not a sensitive function of the bulk electron density. At approximately 160 ns, multistep ionization begins to significantly contribute to the rate of ionization. At this time, both power deposition and the rate of increase in electron density become functions of the bulk electron density. Since n_e and E are not spatially uniform, this mode of power deposition is unstable and leads to the arclike termination of the discharge indicated in the last three frames of Figs. 2 and 3. The constriction shown in Fig. 2 is not a true arc since the gas density in the core is not rarified. The con-

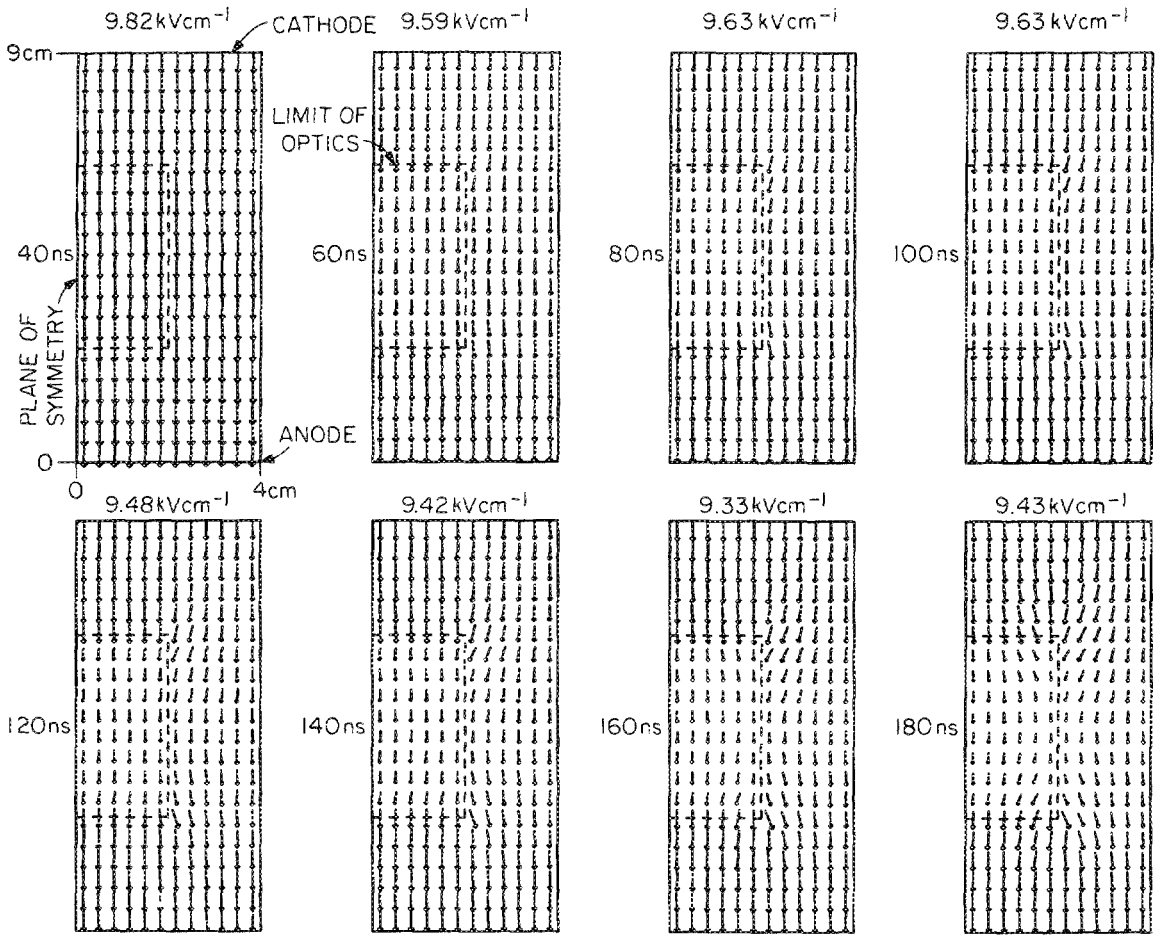

FIG. 3. Electric field vectors for the conditions in Fig. 2 for various times after the start of the current pulse. The lengths of the arrows are measures of the relative strength of the local electric field for the indicated maximum value.

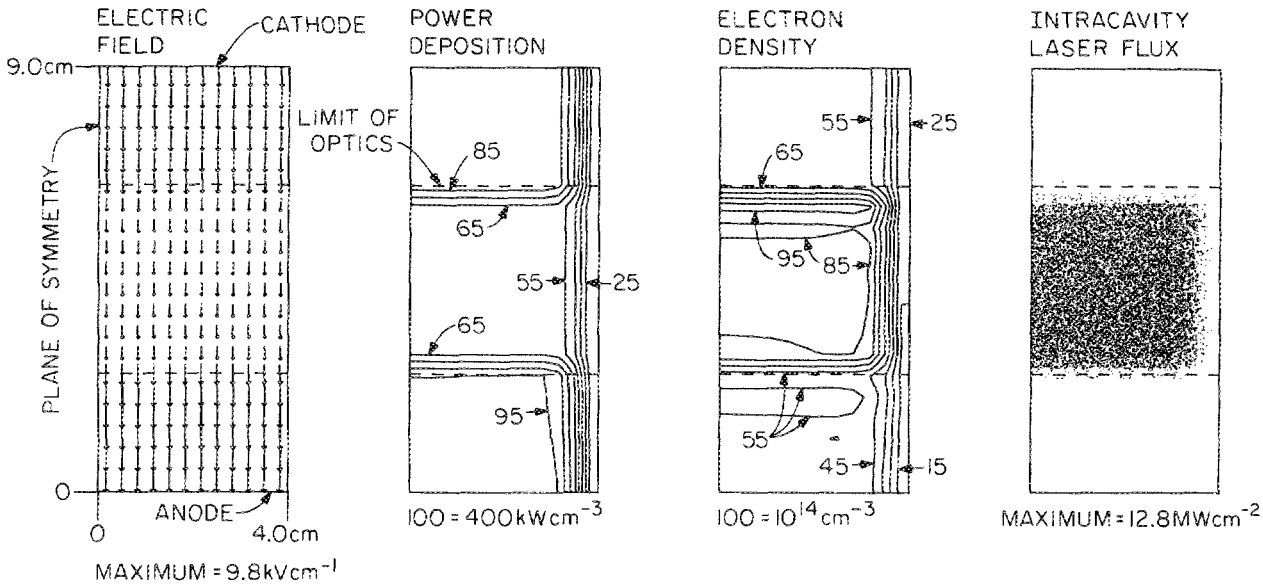

FIG. 4. Electric field vectors, total power deposition (*e* beam and discharge), electron density, and intracavity laser flux for a stable discharge configuration with nonuniform laser extraction. The laser mirrors are rectangular, and centered between and parallel to the discharge electrodes. Laser oscillation is restricted to the volume within the dotted lines. The gradient in conductivity due to photogenerated electrons is parallel to the bulk electric field.

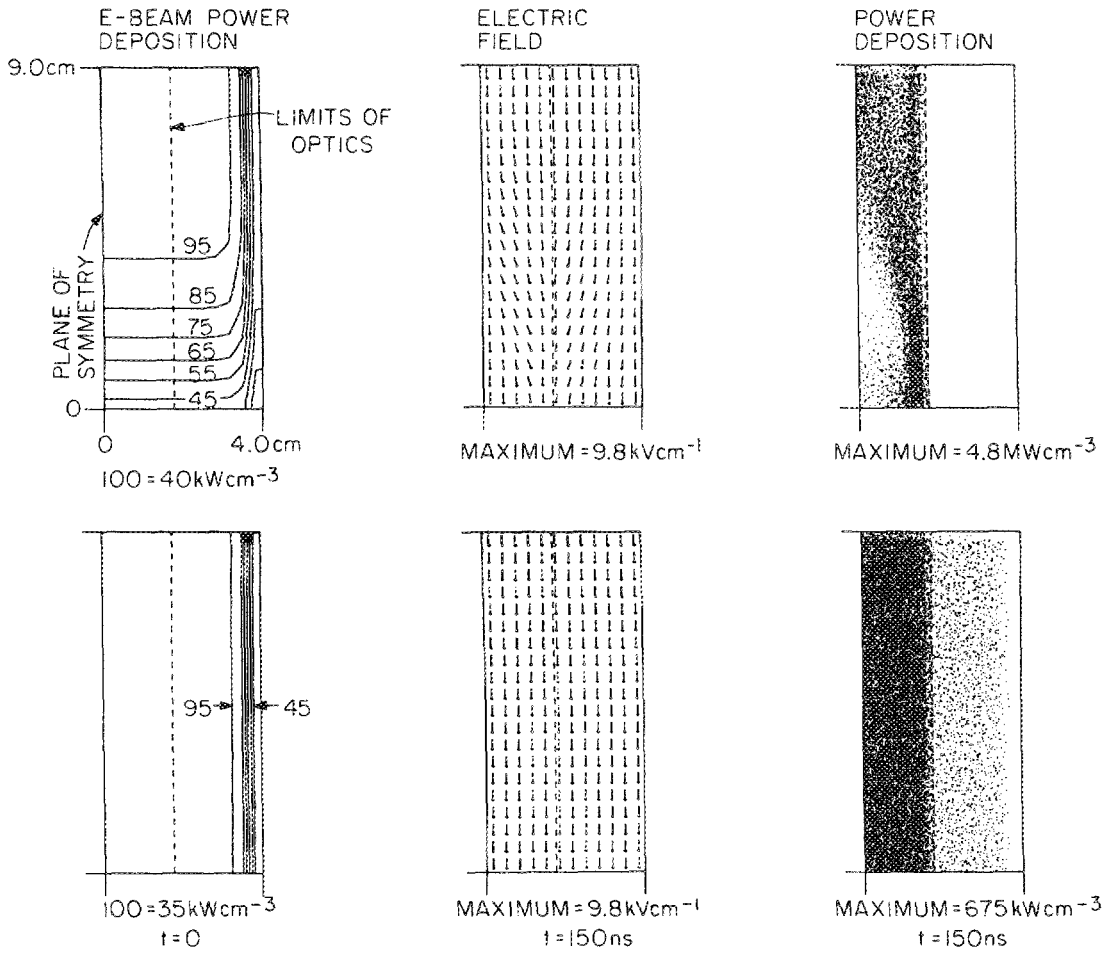

FIG. 5. Unstable (top) and stable (bottom) discharge configurations where the laser mirrors are rectangular, aligned along the centerline, and perpendicular to the electrodes. Laser oscillation is restricted to the volume within the dotted lines. In the unstable configuration the *e* beam is efficiently utilized and the discharge enhancement factor is large, but the criterion that $\nabla\sigma\cdot\mathbf{E} = 0$ is violated. The stable configuration does not violate this criterion but the discharge enhancement factor is small because only a small faction of the total *e*-beam power is deposited in the gas.

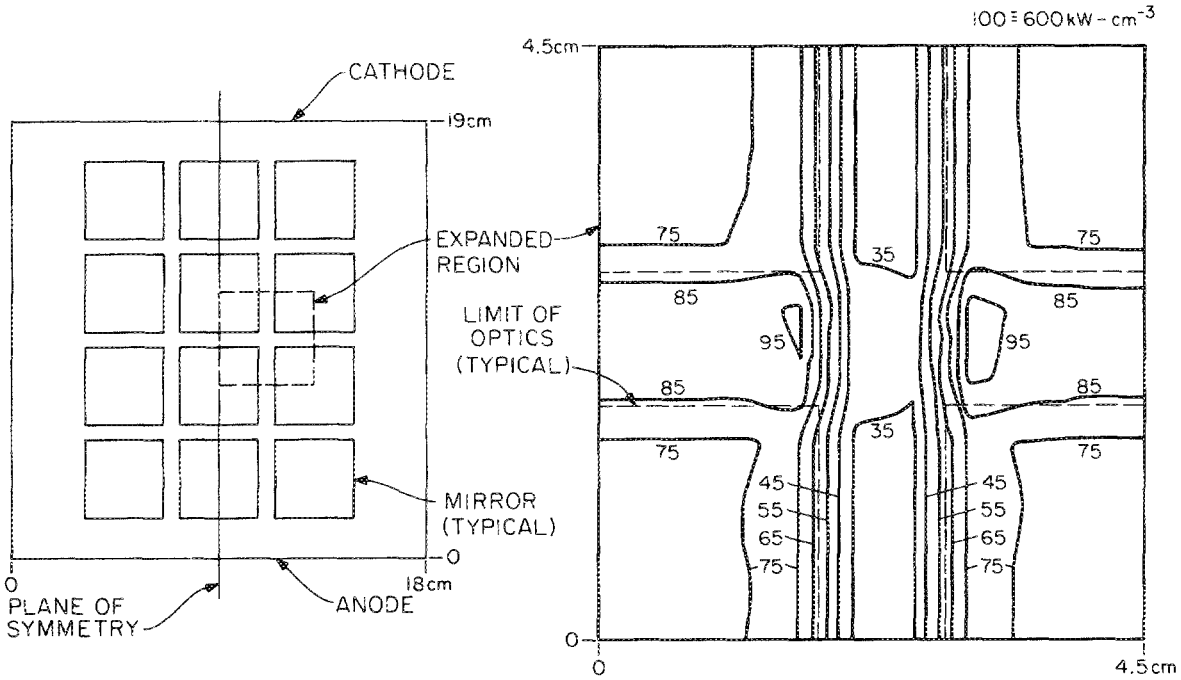

FIG. 6. Total power deposition (*e* beam and discharge) early during the current pulse ($t = 55$ ns) for an EBSD KrF laser using an "eggcrate" configuration for the laser mirrors. The discharge aperture is 19 cm (gap) × 18 cm (width). The mirror arrangment is shown in the sketch, and power deposition is shown for the indicated position of the discharge volume.

striction is rather a local power and ionization instability which will eventually develop into a true arc.

A stable configuration with nonuniform laser extraction can be obtained by insuring that the gradient in conductivity is either perpendicular or parallel to the bulk electric field. The latter criterion is demonstrated in Fig. 4. In this example the laser extraction volume is limited to a strip parallel to the electrodes by having mirrors overlapping the middle third of the discharge. The spatial distribution of electric field, power deposition, and electron density, shown in Fig. 4 at 150 ns into the current pulse, are in a stable configuration. The decrease in power deposition and electron density at the edge of the discharge is defined by the spatial extent of the *e* beam. The electric field and power deposition within the extraction volume are approximately two thirds that of the exterior. The larger electron density near the top of the extraction region is a consequence of a higher rate of *e*-beam power deposition nearer the cathode.

EBSD KrF lasers have been unable to operate with discharge enhancements as large as the theoretical limit. Typically, discharge enhancement values of 2–4 are reported,[3] whereas theory suggests values of 5–8 should be possible.[1,3,6] The cause for this behavior may be, in part, explained by Fig. 5 where *e*-beam power deposition, electric field, and total power deposition are plotted for two distributions of *e*-beam power. In both examples, the laser extraction volume is perpendicular to the electrodes and along the axis of the discharge. In the first example, the *e* beam is efficiently utilized because the majority of the *e*-beam power is deposited in the gas. This configuration has a large discharge enhancement, but the power deposition is not uniform. In the second example, the *e*-beam is not efficiently utilized because the beam electrons traverse the discharge volume and collide with the anode. The *e*-beam power deposition is uniform, but the effective discharge enhancement is low due to the wasted *e*-beam power. The latter example, having low discharge enhancement, is a stable configuration because $\nabla\sigma\cdot\mathbf{E} = 0$. The former example suffers an arclike ionization instability because this criterion is violated.

As the apertures of *e*-beam pumped lasers have increased to a meter or more in size, the mirrors have been segmented in an "eggcrate" configuration.[16] Laser extraction is therefore nonuniform. If an "eggcrate" mirror configuration is used for a large aperture EBSD KrF lasers, local ionization instabilities could occur. To demonstrate this possibility, power deposition is plotted in Fig. 6 early during the current pulse for an EBSD KrF laser using an eggcrate mirror. The conductive channels defined by the columns of mirrors divert power from the volume between the columns. Electric field enhancement at the corners of the mirrors, and in the unextracted volume in the rows between the mirrors, increases power deposition in those areas. To delay the onset of instabilities initiated by such nonuniform power deposition, the separation between mirrors must be as small as possible.

V. CONCLUDING REMARKS

Nonuniform laser extraction in *e*-beam sustained discharge KrF lasers has been identified as an initiating source of local ionization instabilities which terminate the current pulse in an arclike fashion. An intracavity laser flux of approximately the laser saturation flux is large enough to perturb the plasma conductivity, and hence electric field, by

increasing the electron density through photodetachment and photoionization. If nonuniform, this perturbation becomes spatially unstable when multistep ionization begins to compete with ionization by the e beam. This instability can be minimized by insuring that gradients in conductivity due to photogenerated electrons are either parallel or perpendicular to the bulk electric field.

[1]J. D. Daugherty, J. A. Mangano, and J. H. Jacob, Appl. Phys. Lett. **28**, 581 (1976).
[2]J. H. Jacob and J. A. Mangano, Appl. Phys. Lett. **28**, 724 (1976).
[3]M. Rokni, J. A. Mangano, J. H. Jacob, and J. C. Hsia, IEEE J. Quantum Electron. **QE-14**, 464 (1978).
[4]R. T. Brown and W. L. Nighan, Appl. Phys. Lett. **32**, 730 (1978).
[5]W. L. Nighan, IEEE J. Quantum Electron. **QE-14**, 714 (1978).
[6]W. H. Long, J. Appl. Phys. **50**, 168 (1979).
[7]R. T. Brown and W. L. Nighan, Appl. Phys. Lett. **35**, 142 (1979).
[8]R. A. Haas, *Applied Atomic Collisions Physics, Vol. 3: Gas Lasers*, edited by E. W. McDaniel and W. L. Nighan (Academic, New York, 1982), pp. 423–452.
[9]J. Coutts and C. E. Webb, J. Appl. Phys. **59**, 704 (1986).
[10]J. A. Mangano and J. H. Jacob, Appl. Phys. Lett. **27**, 495 (1975).
[11]R. K. Steunenberg and R. C. Vogel, J. Am. Chem. Soc. **78**, 901 (1956).
[12]T. H. Johnson and A. M. Hunter, J. Appl. Phys. **51**, 2406 (1980).
[13]H. A. Hyman, Appl. Phys. Lett. **31**, 14 (1977).
[14]M. J. Kushner and A. L. Pindroh, J. Appl. Phys. **60**, 904 (1986).
[15]W. F. Ames, *Numerical Methods for Partial Differential Equations*, 2nd ed. (Academic, New York, 1977), pp. 114–135.
[16]L. A. Rosocha, P. S. Bowling, M. D. Burrows, M. Kang, J. Hanlon, J. McCleod, and G. W. York, Jr., Laser Part. Beams **4**, 55 (1986).